The role of Mn in photorefractive $LiNbO_3$

Yunping Yang
Department of Electrical Engineering, California Institute of Technology, Pasadena, CA 91125
yunping@sunoptics.caltech.edu

Ali Adibi
School of Electrical and Computer Engineering, Georgia Institute of Technology, Atlanta, Georgia 30332-0250
adibi@ece.galtech.edu

Dirk Berben, Karsten Buse
Universität Bonn, Physikalisches Institut, Wegelerstraβe 8, D-53115 Bonn, Germany
dberben@rz.uni-osnabrueck.de, kbuse@uni-bonn.de

Demetri Psaltis
Department of Electrical Engineering, California Institute of Technology, Pasadena, CA 91125
psaltis@sunoptics.caltech.edu

Abstract: The dynamic range, sensitivity and dark decay of holographic recording in $LiNbO_3$ crystals doped with 0.2 atomic% Mn with different oxidation states have been measured. The sensitivity is 0.5 cm/J and found to be independent of the oxidation states, while the largest *M*/# obtained is 12/mm (extraordinary light polarization, light wavelength 458 nm). The dark decay time constants of non-fixed holograms stored in these $LiNbO_3$:Mn crystals obey an Arrhenius-type dependence on the absolute temperature with an activation energy of about 1.0 eV, and the dark decay is several orders of magnitude slower than that of $LiNbO_3$:Fe with comparable doping levels. In contrast to $LiNbO_3$:Fe, the dominant dark decay mechanism in highly-doped $LiNbO_3$:Mn crystals is due to proton compensation rather than electron tunneling.

OCIS codes: (090.2900) Holographic recording materials; (090.7330) Volume holographic gratings; (210.0210) Optical data storage; (160.3730) Lithium niobate

Introduction

Photorefractive lithium niobate crystals have been intensively investigated for applications such as holographic data storage [1] and narrow-band wavelength filters for optical telecommunications [2-4]. Two of the most important properties of photorefractive $LiNbO_3$ crystals are dopant and doping level. Usually, transition metal dopants, such as Fe, Cu, Ce and Mn, are added to the melt as oxides to improve the photorefractive effect. Among all kinds of dopants, Fe has been investigated extensively, while Mn has been less popular and a lot of efforts have yet to be made to understand its role in $LiNbO_3$ completely. One of the few facts known about Mn in $LiNbO_3$ crystals is that the Mn center is deeper than the Fe center, which has been employed in doubly doped $LiNbO_3$:Fe:Mn to achieve non-volatile holographic storage [5].

In order to get large dynamic range and sensitivity, highly-doped crystals are desirable. Although $LiNbO_3$:Fe crystals have been widely used, one of the drawbacks is the fast dark decay in crystals with

OSA TOPS Vol. 62 Photorefractive Effects, Materials, and Devices
D. Nolte, G. Salamo, A. Siahmakoun, and S. Stepanov, eds.

©2001 Optical Society of America

doping levels above 0.1 wt% Fe_2O_3. For example, the lifetimes of non-fixed holograms in $LiNbO_3$ doped with 0.25 wt% Fe_2O_3 at room temperature are several minutes, which is generally too short for practical applications. This dark decay limits the highest practical doping levels and hence dynamic range and sensitivity. It is desired to have highly doped crystals with acceptable dark decay.

We have found that the dark decay time constants of non-fixed holograms in highly-doped $LiNbO_3$:Mn crystals at room temperature are several orders of magnitude larger than those of $LiNbO_3$:Fe crystals with comparable doping levels. This fact allows us to use $LiNbO_3$:Mn crystals with higher doping levels to get larger *M*/# [6] and higher sensitivity without reducing the hologram lifetime. The measured sensitivity in these $LiNbO_3$:Mn crystals is 0.5 cm/J (extraordinary light polarization, light wavelength 458nm) and is independent of oxidation states, which is unusual for $LiNbO_3$:Fe crystals, while the largest *M*/# obtained in $LiNbO_3$:Mn is 12/mm for strong oxidization.

Lifetimes of non-fixed holograms

Two of the investigated samples are S1, a $LiNbO_3$ crystal doped with 0.2 atomic% Mn, and S2, a $LiNbO_3$:Fe crystal doped with 0.25 wt% Fe_2O_3. The dimensions of the samples S1 and S2 are $4.5\times4.0\times1.0$ mm^3 and $5.0\times3.0\times1.0$ mm^3, respectively. The c-axis is parallel to the longest direction. The crystals are proton-reduced by annealing treatment. In the measurements of the dark decay, the crystals were placed on a heatable plate that was temperature-controlled within 0.1° C accuracy. An argon-ion laser beam with wavelength 514 nm was used to record holograms. The laser beam was split into two extraordinarily polarized beams of equal intensity, that were expanded to cover the whole crystal during recording. Recorded holograms had a grating period of 1.3 μm and were written with the grating vector oriented along the c-axis. Recording was performed at room temperature. Afterwards, the crystals were heated to a certain temperature in the dark and a weak laser beam of 514 nm was used to monitor the holographic diffraction efficiency. The weak readout light illuminated the crystal only from time to time, and the intervals between two measurements were long enough to keep the erasure of the holograms by the probing beam negligible. After each experiment the crystal was heated to 230° C and kept at this temperature under uniform illumination for about 45 minutes to erase the gratings completely.

The results are shown in Figure 1. We can see that the dark decay time constants in both samples, S1 and S2, obey an Arrhenius-type dependence on the absolute temperature *T*, but with two different activation energies, 1.0 eV and 0.28 eV. The different activation energies explicitly indicate two distinct dominant dark decay mechanisms, which have been identified as proton compensation [7-8] and electron tunneling [9-11], respectively. Generally, both of these two mechanisms contribute to the dark decay in $LiNbO_3$ crystals, but for $LiNbO_3$ crystals with low doping levels, electron tunneling is very weak and the dark decay is dominated by proton compensation. With an increase of the doping levels, the effect of electron tunneling becomes stronger and stronger. In $LiNbO_3$:Fe crystals with doping levels above 0.1 wt% Fe_2O_3, the effect of electron tunneling becomes the dominant dark decay origin and limits the highest practical doping level below 0.1 wt% Fe_2O_3. The probability of electron tunneling is proportional to $\exp[-L(V-E)^{1/2}]$, where *L* is the width of the barrier, *V* is the height of the barrier, and *E* is the energy of the electrons. Since the Mn center is deeper than the Fe center, the height of the barrier of Mn center should be larger than that of the Fe center. We would expect that the electron tunneling effect in $LiNbO_3$:Mn crystals is smaller. Figure 1 shows exactly what we expect. The effect of electron tunneling in sample S1 is negligible and the dark decay is still dominated by proton compensation. The activation energy 1.0 eV is typical for this process [7-8]. Actually, we extrapolated dark decay time constants of non-fixed holograms in sample S1 at room temperature to be about 500 days, while the measured lifetime of non-fixed holograms in sample S2 is just several minutes at room temperature.

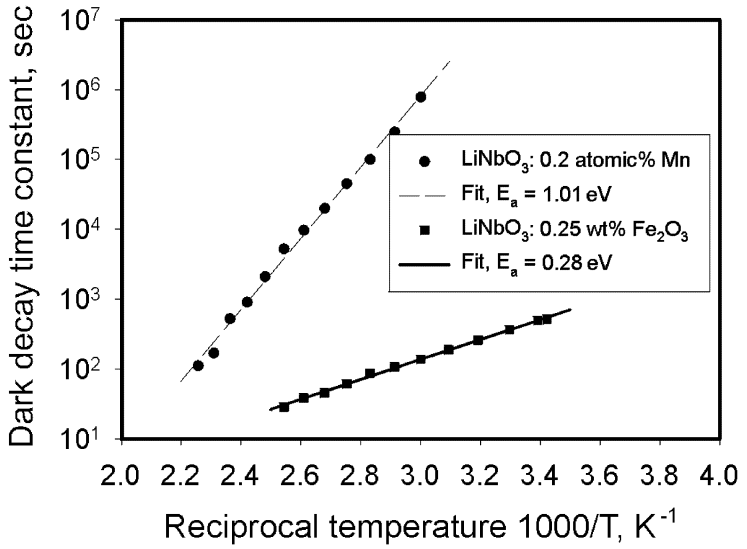

Fig. 1. Arrhenius plot of the dark decay time constants of non-fixed holograms stored in sample S1: $LiNbO_3$ doped with 0.2 atomic% Mn, and in sample S2: $LiNbO_3$ doped with 0.25 wt% Fe_2O_3.

M/# and sensitivity

The Mn center is deeper than the Fe center. In order to make full use of the gain of doping level in $LiNbO_3$:Mn for boosting *M*/# and sensitivity, it is reasonable to use laser light with shorter wavelength. In our experiments of measuring *M*/# and sensitivity, an argon-ion laser beam with the wavelength 458 nm was used to record and to erase holograms. The crystal was placed on a rotation stage. The laser beam was split into two extraordinarily polarized beams of equal intensity, that were expanded to cover the whole crystal during recording and erasure. The intensity of each beam is about 10 mW/cm^2, and the grating vector is aligned along the c-axis with a period length of 1.1 μm. During recording, one beam was blocked from time to time to measure the holographic diffraction efficiency. We used Bragg-mismatched erasure, i.e., during erasure the sample was rotated away from the Bragg-matched position and illuminated by the same two beams that were used to record the holograms. In order to avoid building another very strong hologram and fanning, the sample was rotated 0.02 degree every 10 seconds during erasure. At the end of each period of erasure, the diffraction efficiency was measured by scanning over some range of angle which covered the Bragg-matched position with only the reference beam on. A typical recording and erasure curve for sample S1 is shown in Figure 2. From single-hologram recording and erasure, we obtain a sensitivity of about 0.5 cm/J and an *M*/# of 6.5/mm. Here the sensitivity is defined as $S = (\mathrm{d}\eta^{1/2}/\mathrm{dt})|_{t=0}/IL$, and the *M*/# is defined as $M/\# = (\mathrm{d}\eta^{1/2}/\mathrm{dt})|_{t=0}\times\tau_e$, where η is the diffraction efficiency calculated as $I_{\mathrm{diffracted}}/I_{\mathrm{incident}}$, L is the thickness of the crystal, I is the total intensity of the recording beams, and τ_e is the erasure time constant. Notice that both, S and *M*/#, are pretty high compared to the typical values of $LiNbO_3$:Fe, which are 0.1 cm/J and 1/mm, respectively.

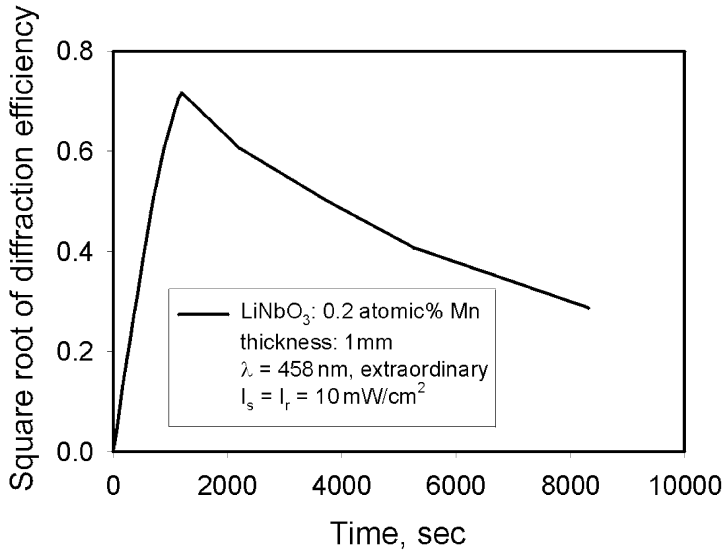

Fig. 2. Typical recording and erasure curve for sample S1: $LiNbO_3$ doped with 0.2 atomic% Mn.

Multiplexing 100 holograms

In order to verify that the *M*/# is real and achievable for practical applications, 100 holograms have been multiplexed in sample S1 (extraordinary light polarization, light wavelength 458 nm). Figure 3 shows the comb function of the 100 multiplexed holograms. We used a pre-calculated exposure schedule to equalize the diffraction efficiency. The angle between two neighboring holograms is 0.4 degrees. The *M*/# we got from this multiplexing, which was calculated by $M/\# = \Sigma\eta_n^{1/2}$, is 5.0/mm, where η_n is the diffraction efficiency of the n^{th} hologram. The loss of some *M*/# is due to the non-ideal exposure schedule [6]. The larger diffraction efficiencies around the center of the comb function are due to some back reflection. The *M*/#'s obtained from both -- single-hologram recording and erasure, and multiplexing -- agree very well.

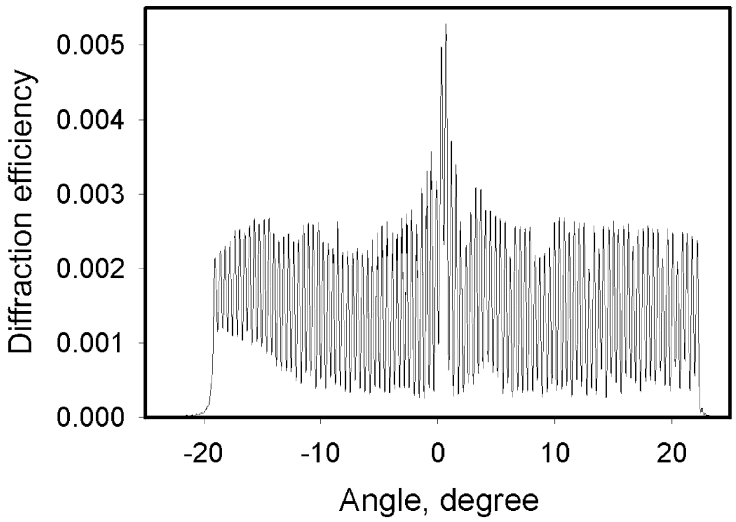

Fig. 3. Comb function of multiplexing 100 holograms in sample S1: $LiNbO_3$ doped with 0.2 atomic% Mn. The *M*/# calculated from this comb function is 5.

M/# and sensitivity vs oxidation state

The oxidation state of $LiNbO_3$ crystals can be changed by annealing at elevated temperature in appropriate atmosphere, typically oxygen for oxidation and argon for reduction. It is well known that *M*/# and sensitivity in $LiNbO_3$:Fe crystals are strong functions of oxidation state. Typically, the more the crystal is reduced, the larger the sensitivity and the smaller the *M*/#, and vice versa. We also measured *M*/# and sensitivity in sample S3, a $LiNbO_3$ crystal doped with 0.2 atomic% Mn, with different oxidation states. Sample S3 was cut from the same boule as S1 and was also proton-reduced and with the same size as sample S1. Table 1 contains information about the thermal treatment for each oxidation state. Since the absorption band of the Mn center is very wide, it is very hard to determine the ratio of $C_{Mn^{2+}}/C_{Mn^{3+}}$ quantitatively. The measured *M*/#'s and sensitivities for different oxidation states are shown in Figure 4. Surprisingly, the sensitivity in sample S3 is almost the same, 0.5 cm/J, and it is almost independent of the oxidation states, while the *M*/# drops by a factor of 15 from the highly oxidized to the highly-reduced state. The highest *M*/# was obtained for the highly-oxidized state. We suspect that the sensitivity for highly-oxidized states does not drop as one might expect is probably because holes play a significant role in photorefractive recording. Another implication of the fact that the highly-oxidized state is the optimal oxidation state (in terms of sensitivity and *M*/#) in $LiNbO_3$:Mn is that we can use even higher doping levels without losing the advantage of the slow dark decay. This is because the electron tunneling effect is proportional to the effective trap concentration $C_{Mn^{2+}}C_{Mn^{3+}}/(C_{Mn^{2+}}+C_{Mn^{3+}})$, which is approximately equal to the concentration of $C_{Mn^{2+}}$ for highly-oxidized $LiNbO_3$:Mn, and therefore very small.

Table 1. Summary of oxidation states of sample S3

Oxidation state	Thermal treatment
State 1	highly-oxidized, starting with state 6, in oxygen at 930°C for 24 hours.
State 2	starting with state 1, in argon at 780°C for 1 hour.
State 3	starting with state 2, in argon at 780°C for 3 hours.
State 4	starting with state 3, in argon at 780°C for 4 hours.
State 5	starting with state 4, in argon at 780°C for 11 hours.
State 6	highly-reduced, in vacuum at 1000°C for 14 hours, then in oxygen at 925°C for 4 hours.

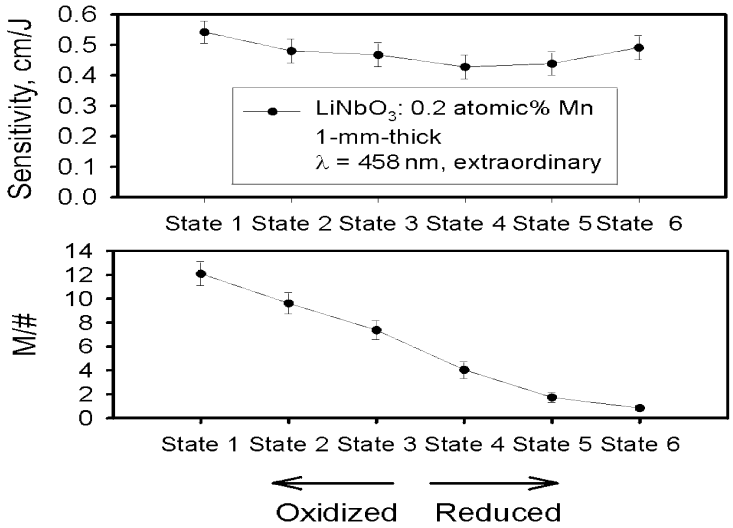

Fig. 4. Measured sensitivity and *M*/# vs. oxidation state in sample S3: $LiNbO_3$ doped with 0.2 atomic% Mn.

Conclusions

In summary, we have shown that $LiNbO_3$:Mn crystals are very promising for holographic recording. The dominant dark decay effect in highly-doped $LiNbO_3$:Mn crystals, which is due to ionic compensation, is smaller than that in $LiNbO_3$:Fe crystals with comparable doping levels, where electron tunneling dominates the dark decay. The measured sensitivity of one of the $LiNbO_3$ crystals doped with 0.2 atomic% Mn is 0.5 cm/J and almost independent of the oxidation state, while the highest *M*/# measured is 12/mm for strong oxidization. The fact that the optimal oxidation state is that of high oxidization allows us to use even higher doping levels in $LiNbO_3$:Mn crystals yielding even larger *M*/#'s and sensitivities, since the effect of electron tunneling is much smaller in highly-oxidized crystals. Several open questions remain concerning the role of Mn in the photorefractive effect in $LiNbO_3$. These include the origin of the high *M*/# measured and the fact that the sensitivity does not depend strongly on the oxidation/reduction state.

Acknowledgments

Effort sponsored by NSF, Center for Neuromorphic Systems Engineering ERC and DARPA. The authors thank the NSF and the DAAD for sponsoring the US-German collaboration. We thank Ingo Nee for fruitful discussions.

References

1. H. J. Coufal, D. Psaltis and G. T. Sincerbox, *Holographic Data Storage*, Springer (2000).
2. V. Leyva, G. A. Rakuljic, and B. O'Conner, "Narrow bandwidth volume holographic optical filter operating at the Kr transition at 1547.82 nm", Appl. Phys. Lett. 65, 1079-1081 (1994).
3. R. Müller, M. T. Santos, L. Arizmendi, and J. M. Cabrera, "A narrow-band interference filter with photorefractive $LiNbO_3$," J. Phys. D 27, 241-246 (1994).
4. S. Breer, H. Vogt, I. Nee, and K. Buse, "Low-crosstalk WDM by Bragg diffraction from thermally fixed reflection holograms in lithium niobate," Electron. Lett. 34, 2419-2421 (1998).
5. K. Buse, A. Adibi, and D. Psaltis, "Non-volatile holographic storage in doubly doped lithium niobate crystals," Nature. 393, 665-668 (1998).
6. F. Mok, G. Burr, and D. Psaltis, "System metric for holographic memory systems," Opt. Lett. 21, 896-898 (1996).
7. D. L. Staebler and J. J. Amodei, "Thermally fixed holograms in $LiNbO_3$," Ferroelectrics 3, 107-113 (1972).
8. A. Yariv and S. Orlov, "Holographic storage dynamics in lithium niobate: theory and experiment," J. Opt. Soc. Am. B 13, 2513-2523 (1996).
9. I. B. Barkan, A. V. Vorob'ev, and S. I. Marennikov, "Transient optical storage in lithium niobate crystal," Sov. J. Quantum Electron. 9, 492-494 (1979).
10. I. Nee, M. Müller, K. Buse, and E. Krätzig, "Role of iron in lithium-niobate crystals for the dark-storage time of holograms," J. Appl. Phys. 88, 4282-4286 (2000).
11. Y. Yang, I. Nee, K. Buse, and D. Psaltis, "Ionic and Electronic Dark Decay of Holograms in $LiNbO_3$:Fe Crystals," Appl. Phys. Lett., (Accepted for the version of June 18, 2001).